Electronic Materials Letters, Vol. 6, No. 3 (2010), pp. 117-121
DOI: 10.3365/eml.2010.09.117 Published 30 September 2010

Microstructures and Thermoelectric Properties of Spark Plasma Sintered In_4Se_3

Young Soo Lim,[1] Ja Young Cho,[1,2] Jae-Ki Lee,[1,2] Soon-Mok Choi,[1] Kyoung Hun Kim,[1] Won-Seon Seo,[1,*] and Hyung-Ho Park[2]

[1]Green Ceramics Division, Korea Institute of Ceramic Engineering and Technology, 233-5 Gasan-dong, Geumcheon-gu, Seoul 153-801, Korea
[2] Department of Materials Science and Engineering, Yonsei University, 134 Sinchon-dong, Seodaemun-gu, Seoul 120-749, Korea

We report microstructures and thermoelectric properties of In_4Se_3 thermoelectric materials. In_4Se_3 powder was synthesized by conventional melting process in evacuated quartz ampoules and sintering of In_4Se_3 was performed by spark plasma method at various sintering temperature. The microstructure and density of the sintered body of In_4Se_3 were strongly dependent on the sintering temperature. Thermoelectric properties, such as electrical conductivity, Seebeck coefficient and thermal conductivity, were also characterized and the effects of the sintering condition on the thermoelectric properties were investigated.

Keywords: thermoelectric materials, sintering, conductivity, x-ray diffraction, In_4Se_3.

1. INTRODUCTION

Recently, thermoelectric power generation from waste heat has been attracted much attention due to the global issues on energy demand and climate change. For the energy conversion from waste heat into electricity, thermoelectric material plays a key role by Seebeck effect. The performance of the thermoelectric material is quantified by dimensionless figure of merit, $ZT = S^2\sigma T/k$, where S, σ, T, and k are the Seebeck coefficient, electrical conductivity, absolute temperature and thermal conductivity, respectively.

In_4Se_3 has received considerable attention because of its high thermoelectric performance.[1-3] In_4Se_3 has a space group of $D2h^{12}$–P_{nnm} and it is composed of quasi 2 dimensional covalent bond layers and quasi 1 dimensional In chains.[4,5] This low dimensional nature in the In_4Se_3 lattice leads to unique lattice imperfections, such as Peierls distortion and condenson.[1,6,7] These imperfections could restrain the thermal conduction in the lattice by phonon scattering, so that In_4Se_3 shows a high thermoelectric figure of merit, ZT.

For the densification of In_4Se_3 thermoelectric material, spark plasma sintering and hot pressing have been used.[2,3] Because In-Se system has many kinds of binary compound phases, such as InSe, In_2Se_3, In_4Se_3, In_5Se_6 and In_6Se_7, the sintering condition is of great concern to avoid unintentional phase transformation during the sintering process of In_4Se_3 powder.[8-10] However, there has been no report on the effect of the sintering condition on the thermoelectric properties of In_4Se_3.

In this study, we report the effect of the sintering temperature on the structural and thermoelectric properties of the spark plasma sintered In_4Se_3. To investigate the phase transformation from In_4Se_3 to any In-Se binary phase during the sintering process, structural characterizations of the samples sintered at various sintering temperatures were carried out by using a scanning electron microscope and an x-ray diffractometer. Dependency of the thermoelectric properties on the sintering condition was also investigated and the results were discussed.

2. EXPERIMENTAL DETAILS

In and Se raw materials were melted in evacuated quartz ampoules by induction furnace to prepare In-Se ingot. For n-type self-doping, the nominal composition of In-Se ingot was controlled to $In_4Se_{2.5}$. Two-step annealing of In-Se ingot was carried out for the evolution of homogeneous In_4Se_3 phase at 808 K for 48 h and 703 K for 24 h, respectively. The annealed ingot was pulverized into powder (8 - 30 μm) and the phase was examined by using an x-ray diffractometer (XRD, Rigaku, Japan). The result showed that In_4Se_3 phase was successfully synthesized by the two-step annealing. Sintered bodies of the In_4Se_3 powder were prepared by spark plasma sintering (SPS-515S, Sumitomo Coal Mining) under uniaxial pressure of 70 MPa for 5 min at 523 K, 573 K, 663 K and 693 K. The density of the sintered body was analyzed by Archimedes method and their microstructures were char-

*Corresponding author: gglee@pknu.ac.kr

acterized by using a scanning electron microscope (SEM, JSM-6700, JEOL). Electrical conductivity and Seebeck coefficient were characterized by a four point probe method using a thermoelectric measurement system (RZ-2001i, Ozawa Science) and thermal conductivity was measured by using a laser flash method (LFA-457, NETZSCH).

3. RESULTS AND DISCUSSION

Figure 1(a) shows powder XRD patterns of In_4Se_3 before and after spark plasma sintering. As-prepared In_4Se_3 powder sample (Reference) showed a sharp diffraction pattern, and main diffraction peaks of (330), (311) and (002) were clearly observed before the sintering process. After sintering at relatively low temperatures (523 K and 573 K), InSe second phase was detected in the sintered body of In_4Se_3 powder. It indicates that unintended phase transformation from In_4Se_3 to InSe was induced by the spark plasma sintering. However, in the samples sintered at higher temperatures (663 K and 693K), the InSe second phase disappeared. InSe is the most stable structure at low temperature among various In-Se compounds, so that the sintering at higher temperature could suppress the formation of the InSe second phase.[10]

Because the spark plasma sintering was performed under uniaxial pressure of 70 MPa, the sintered body of In_4Se_3 could show the preferred direction. Figure 1(b) shows the relative peak-to-peak intensities of I_{330}/I_{002} and I_{311}/I_{002} calculated from the diffraction peaks of In_4Se_3 in Fig. 1(a). After the sintering process, both of the relative peak-to-peak intensities were significantly reduced. It means that the diffraction from (*hk*0) or (*hkl*) plane became weaker and that from (00*l*) plane became stronger after the sintering. Because of its anisotropic layered crystal structure of In_4Se_3 (a_o = 15.296, b_o = 12.308, c_o = 4.081 Å), it is quite reasonable that <00*l*> direction became parallel to the axis of the pressure.[5]

Figures 2(a) to (d) shows SEM micrographs of fractured surface of In_4Se_3 sintered at 523 K, 573 K, 663 K and 693 K, respectively. As shown in Fig. 2(a) and (b), large amount of fragmented particles was observed in the samples sintered at relatively low temperature. It indicates that those samples were not fully densified at low sintering temperature. However, with increasing the temperature, large sintered grains of In_4Se_3 (bigger than 10 μm) became dominant in the samples. The fractured surfaces of the grains showed step-like shape and it might be originated from the layered structure of In_4Se_3.[4,5]

The densities of the sintered bodies were characterized by Archimedes method and the results are shown in Fig. 3. The density of the sample sintered at 523 K was 4.757 g/cm^3 and the relative density was only 79%. Therefore, the easily fragmented structure in Fig. 2(a) and (b) might be originated from the poor densification at low sintering temperature. However, the density increased monotonously with increasing temperature. The density of the sample sintered at 693 K (6.026 g/cm^3) was almost the same to the value in Ref. 11.

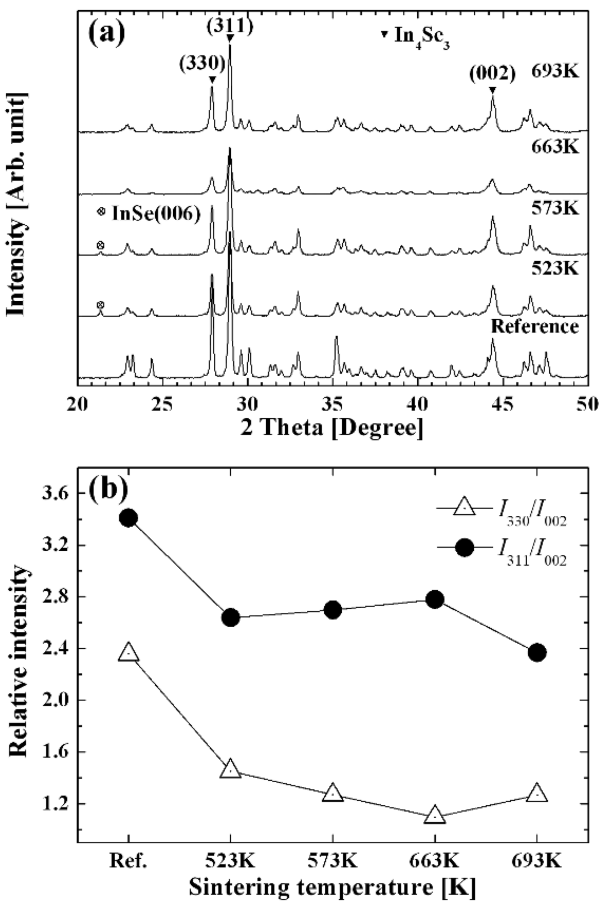

Fig. 1. (a) Powder x-ray diffraction patterns of In_4Se_3 before and after spark plasma sintering and (b) relative peak-to-peak intensities of intensities of I_{330}/I_{002} and I_{311}/I_{002}.

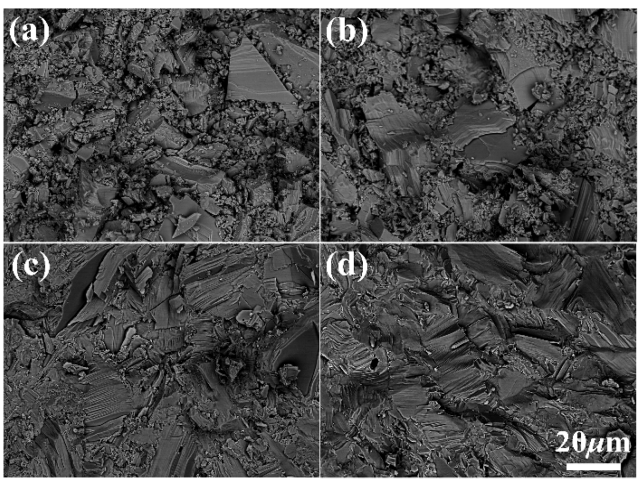

Fig. 2. (a) to (d) SEM micrographs of the fractured surfaces of In_4Se_3 sintered at 523 K, 573 K, 663 K and 693 K, respectively.

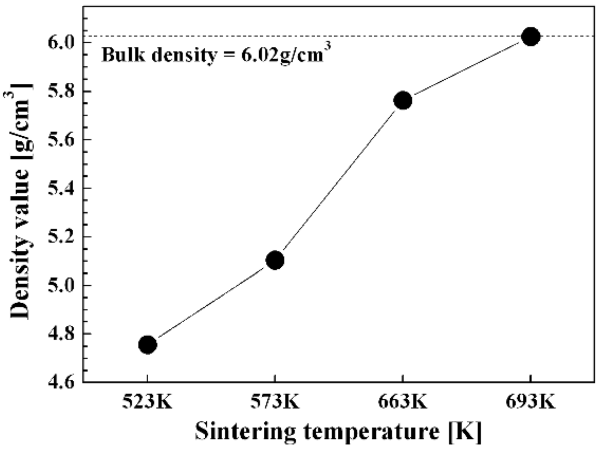

Fig. 3. Density of the sintered In_4Se_3 samples as a function of the sintering temperature.

Figures 4(a) to (c) show electrical conductivity (σ), Seebeck coefficient (S) and power factor ($S^2\sigma$) of the sintered In_4Se_3 samples, respectively. Except for the sample sintered at 523 K, the electrical conductivities were not quite different from each other. Above 465 K, the electrical conductivities exponentially increased with increasing temperature in all samples and the activation energies were within the range from 0.19 eV to 0.27 eV as shown in the inset. In literature, Rhyee *et al.* calculated the direct band gap energy of In_4Se_3 by generalized gradient approximation with spin-orbital interaction.[2] Although the calculated band gap energy was 0.2 eV, the authors expected that actual band gap might be greater than the calculated value, since their model usually provided smaller value than the experimental result. In this experiment, the activation energy of the electrical conductivity was quite compatible to the band gap energy of In_4Se_3, so that the increasing electrical conductivity with measurement temperature could be regarded as the result of the increase of carrier concentration by thermal excitation.

The Seebeck coefficients showed negative values in all samples due to the n-type conduction properties and they were strongly affected by the sintering temperature as shown in Fig. 4(b). The absolute Seebeck coefficients of In_4Se_3 sintered at 523 K and 573 K were less than 10 μV/K up to 400 K of the measurement temperature. However, as the sintering temperature increased, the absolute value of the Seebeck coefficient also increased and the maximum Seebeck coefficient of -281 μV/K was obtained from the sample sintered at 693K.

The power factors ($S^2\sigma$) of the In_4Se_3 samples sintered at various temperatures are shown in Fig. 4(c). The power factor of In_4Se_3 was strongly dependent on the sintering temperature and the sample sintered at higher temperature showed much improved power factor. Monotonic increase of the power factor with increasing measurement temperature was

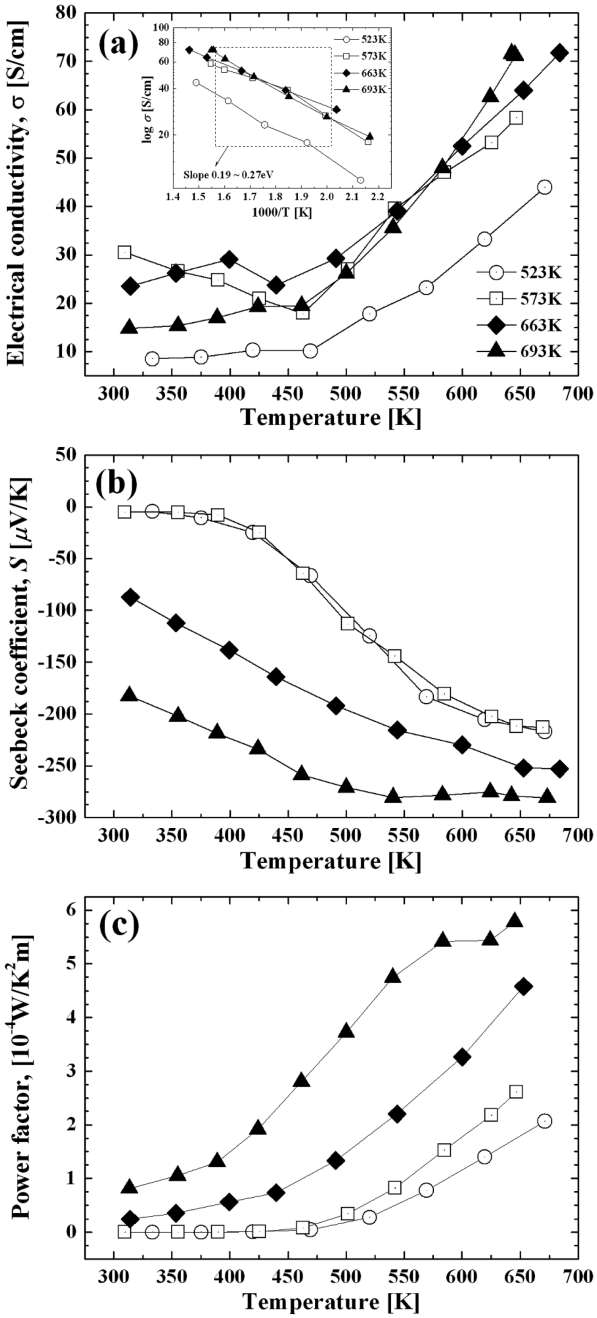

Fig. 4. (a) Electrical conductivity, (b) Seebeck coefficient and (c) power factor of the sintered In_4Se_3 samples as a function of the measurement temperature.

also observed. The maximum power factor of 5.77×10^{-4} W/mK^2 was obtained from the samples sintered at 693 K in this experiment and it was mainly attributed to the enhanced Seebeck coefficient rather than electrical conductivity as shown in Fig. 4(a) and (b).

Figure 5(a) shows thermal conductivity of the sintered In_4Se_3. In this experiment, the samples sintered at low temperature showed slightly lower thermal conductivity than

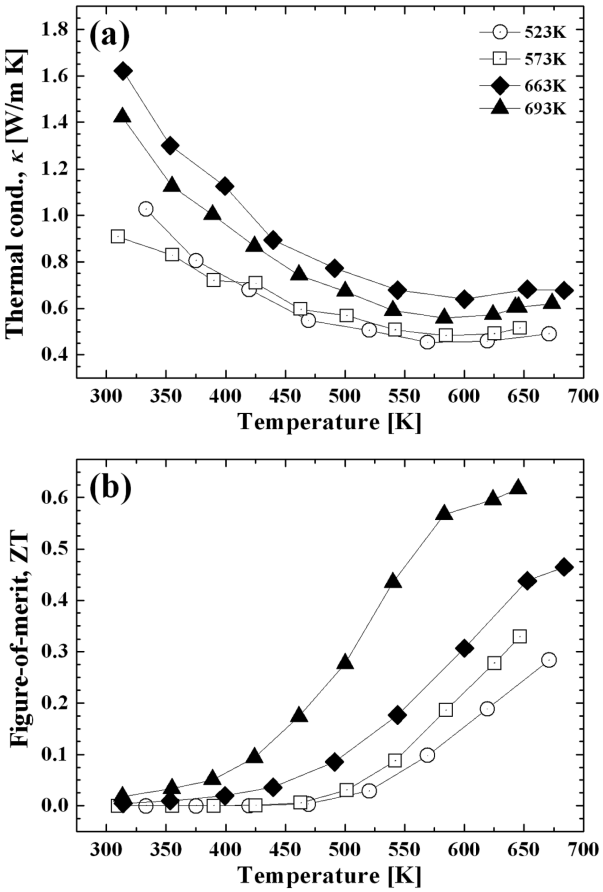

Fig. 5. (a) Thermal conductivity and (b) dimensionless figure of merit of the sintered In_4Se_3 samples as a function of the measurement temperature.

that at high temperature. As shown in Fig. 3, In_4Se_3 sintered at low temperature was not fully densified, so that the density was much smaller than its theoretical value. Therefore, the thermal conduction by phonon could be suppressed due to the imperfection in the samples sintered at low temperature.

It has been reported that Peierls distortion by charge density wave leads to the breakage in the translational symmetry and condenson state by strong electron-phonon interaction induces structural defects in the In_4Se_3 lattice.[1,6,7,12] Therefore, phonon scattering at these defective structure could restrain the thermal conduction. Moreover, the abundant low frequency phonon modes in the In_4Se_3 also influences the thermal conductivity.[5,13] Consequently, In_4Se_3 sintered at high temperature in this experiment could also show the extremely low thermal conductivity (less than 1.0 W/mK) due to its unique features of the low dimensional nature of In_4Se_3 structure.

Figure 5(b) shows the dimensionless figure of merit of the samples. In all samples, the value of *ZT* increased monotonously with measurement temperature. Due to its high power factor in Fig. 4(c), the highest *ZT* of 0.61 at 645 K was obtained in the sample sintered at 693 K. When we consider the measurement temperature, this value is slightly higher that experimental results in Ref. 2 (*ZT* = 0.63 at 710 K) and 3 (*ZT* = 0.6 at 700 K).

4. CONCLUSIONS

In conclusions, we successfully synthesized the In_4Se_3 powder in a single phase by melting and two-step annealing process. The In_4Se_3 powder was densified by spark plasma sintering method at various sintering temperature, and the effect of the sintering condition on the structural and thermoelectric properties of In_4Se_3 were investigated. From the XRD results, it was found that the spark plasma sintering could induce the phase transformation from In_4Se_3 to InSe. Because InSe is unstable at relatively high temperature, we could avoid the formation of the InSe second phase by sintering at high temperature(663 K and 693 K). The effects of the sintering condition on the thermoelectric properties, such as electrical conductivity, Seebeck coefficient, and thermal conductivity, were also characterized, and we could achieve the highest *ZT* of 0.61 at 645 K in the sample sintered at 693 K.

ACKNOWLEDGMENT

This research was supported by a grant from the Fundamental R&D Program for Core Technology of Materials funded by the Ministry of Knowledge Economy, Republic of Korea.

REFERENCES

1. J. -S. Rhyee, K. H. Lee, S. M. Lee, E. Cho, S. I. Kim, E. Lee, Y. S. Kwon, J. H. Shim and G. Kotliar, *Nature* **459**, 965 (2009).
2. J.-S. Rhyee, E. Cho, K. H. Lee, S. M. Lee, S. I. Kim, H. -S. Kim, Y. S. Kwon, and S. J. Kim, *Appl. Phys. Lett*. **95**, 212106 (2009).
3. X. Shi, J. Y. Cho, J. R. Salvador, J. Yang, and H. Wang, *Appl. Phys. Lett*. **96**, 162108 (2010).
4. Y. B. Losovyj, M. Klinke, E. Cai, I. Rodriguez, J. Zhang, L. Makinistian, A. G. Petukhov, E. A. Albanesi, P. Galiy, Y. Fiyala, J. Liu and P. A. Dowben, *Appl. Phys. Lett*. **92**, 122107 (2008).
5. D. M. Bercha and K. Z. Rushchanski, *Phys. Solid State* **40**, 1906 (1998).
6. D. M. Bercha, L. Y. Kharkhalis, A. I. Bercha, and M. Sznajder, *Phys. Stat. Sol*. (b) **203**, 427 (1997).
7. D. M. Bercha, L. Y. Kharkhalis, A. I. Bercha, and M. Sznajder, *Semiconductors* **31**, 1118 (1997).
8. J.-C. Tedenac, G. P. Vassilev, B. Daouchi, J. Rachidi, and G.

Brun, *Cryst. Res. Technol.* **32**, 605 (1997).
9. C. Chatillon, *J. Cryst. Growth* **129**, 297 (1993).
10. G. P. Vassilev, B. Daouchi, M. -C. Record, and J. -C. Tedenac, *J. Alloys Compd.* **269**, 107 (1998).
11. J. H. C. Hogg, H. H. Sutherland, and D. J. Williams, *Acta Crystallogr.* **B 29**, 1590 (1973).
12. L. S. Kukushkin, *Zh. Eksp. Teor. Fiz. Pis'ma* 7, 194 (1968).
13. E. G. Lavut, N. V. Chelovskaya, E. V. Anokhina, V. N. Denim, and V. P. Zlomanov, *J. Chem. Thermodynamics* **27**, 1337 (1995).